EC - Energy and Reserves Dispatch with Distributionally Robust Joint Chance Constraints

Christos Ordoudis, Viet Anh Nguyen, Daniel Kuhn, Pierre Pinson,

This document serves as an electronic companion (EC) for the paper "Energy and Reserves Dispatch with Distributionally Robust Joint Chance Constraints". It contains five sections that provide proofs of the prepositions in the original manuscript, a nomenclature, the robust optimization formulation, data for the IEEE 24-bus RTS and parameters related to the reformulation of distributionally robust chance constraints, as well as additional results.

1. Proofs

Proof of Proposition 1. To ease the notation, we define

$$\hat{a}_k(\xi) := \frac{K}{\epsilon}(B_k Y + C_k)\xi + \frac{K}{\epsilon}(A_k x - b_k) + (1 - \frac{K}{\epsilon})\tau, \tag{1}$$

which is a linear function in ξ. Using standard duality techniques, each worst-case CVaR in

$$\mathcal{Z}^B := \left\{ x, Y : \sup_{\mathbb{Q} \in \mathcal{P}} \text{CVaR}_{\frac{\epsilon}{K}}(A_k x + (B_k Y + C_k)\xi - b_k) \leq 0, \forall k \right\} \tag{2}$$

can be rewritten as

$$\sup_{\mathbb{Q} \in \mathcal{P}} \text{CVaR}_{\frac{\epsilon}{K}}(A_k x + (B_k Y + C_k)\xi - b_k)$$

$$= \sup_{\mathbb{Q} \in \mathcal{P}} \inf_{\tau \in \mathbb{R}} \left\{ \tau + \frac{K}{\epsilon} \mathbb{E}^{\mathbb{Q}} \left[(A_k x + (B_k Y + C_k)\xi - b_k - \tau)^+ \right] \right\} \tag{3a}$$

$$= \sup_{\mathbb{Q} \in \mathcal{P}} \inf_{\tau \in \mathbb{R}} \left\{ \mathbb{E}^{\mathbb{Q}} \left[\max \{ \tau, \hat{a}_k(\xi) \} \right] \right\} \tag{3b}$$

$$\leq \inf_{\tau \in \mathbb{R}} \left\{ \sup_{\mathbb{Q} \in \mathcal{P}} \mathbb{E}^{\mathbb{Q}} \left[\max \{ \tau, \hat{a}_k(\xi) \} \right] \right\}, \tag{3c}$$

where in (3a) we use the definition of CVaR in [1, Theorem 1], and the inequality in (3c) comes from weak duality. Since the Slater's condition holds, the inequality holds with equality. Because the expression inside the expectation is a pointwise maximum of two affine functions in terms of ξ, [2, Corollary 5.1, part (i)] applies and the supremum subproblem over the probability measure $\mathbb{Q}$ in (3c) admits a reformulation in the dual form, and we can rewrite each worst-case CVaR value as

$$\sup_{\mathbb{Q} \in \mathcal{P}} \text{CVaR}_{\frac{\epsilon}{K}}(A_k x + (B_k Y + C_k)\xi - b_k) =$$

$$\begin{cases} \inf_{\tau_k, \lambda_k, s_k, \gamma_k} & \lambda_k \rho + \frac{1}{N} \sum_{i=1}^{N} s_{ik} \\ \text{s.t.} & \tau_k \leq s_{ik} & \forall i \\ & \frac{K}{\epsilon}(A_k x - b_k) + \frac{K}{\epsilon}(B_k Y + C_k)\widehat{\xi}_i \\ & \quad + (1 - \frac{K}{\epsilon})\tau_k + \gamma_{ik}^\top(h - H\widehat{\xi}_i) \leq s_{ik} & \forall i \\ & \| H^\top \gamma_{ik} - \frac{K}{\epsilon}(B_k Y + C_k)^\top \|_* \leq \lambda_k & \forall i \\ & \gamma_{ik} \geq 0 & \forall i, \end{cases} \tag{4}$$

and $\mathcal{Z}^B$ can be reformulated as the intersection of K feasible sets by substituting the value of (4) into (2). This completes the proof. $\square$

Proof of Proposition 2. To ease the notation, we define

$$\bar{a}_k(\xi) := \frac{\alpha_k}{\epsilon}(B_k Y + C_k)\xi + \frac{\alpha_k}{\epsilon}(A_k x - b_k) + (1 - \frac{1}{\epsilon})\tau. \tag{5}$$

For an individual chance constraint from the feasible set

$$\mathcal{Z}(\alpha) := \{x, Y : \mathcal{J}(x, Y, \alpha) \leq 0\}, \tag{6}$$

the worst case CVaR can be expressed based on definition in [1, Theorem 1] as

$$\mathcal{J}(x, Y, \alpha) = \sup_{\mathbb{Q} \in \mathcal{P}} \mathrm{CVaR}_\epsilon \left(\max_k \{\alpha_k (A_k x + (B_k Y + C_k)\xi - b_k)\} \right)$$

$$= \sup_{\mathbb{Q} \in \mathcal{P}} \inf_{\tau \in \mathbb{R}} \left\{ \tau + \frac{1}{\epsilon} \mathbb{E}^{\mathbb{Q}} \left[\left(\max_k \{\alpha_k (A_k x + (B_k Y + C_k)\xi - b_k)\} - \tau \right)^+ \right] \right\} \tag{7a}$$

$$= \sup_{\mathbb{Q} \in \mathcal{P}} \inf_{\tau \in \mathbb{R}} \left\{ \mathbb{E}^{\mathbb{Q}} \left[\max \left\{ \tau, \max_k \bar{a}_k(\xi) \right\} \right] \right\} \tag{7b}$$

$$\leq \inf_{\tau \in \mathbb{R}} \left\{ \sup_{\mathbb{Q} \in \mathcal{P}} \mathbb{E}^{\mathbb{Q}} \left[\max \left\{ \tau, \max_k \bar{a}_k(\xi) \right\} \right] \right\}. \tag{7c}$$

Using the same reasoning as in the proof of Proposition 1, the third inequality holds with equality. The expression inside the expectation is the pointwise maximum of $K+1$ affine functions. Thus, we can reformulate the worst-case functional $\mathcal{J}(x, Y, \alpha)$ based on [2, Corollary 5.1, part (i)] as

$$\mathcal{J}(x, Y, \alpha) =$$
$$\begin{cases} \min_{\tau, \lambda, s} & \lambda \rho + \frac{1}{N} \sum_{i=1}^{N} s_i \\ \mathrm{s.\,t.} & \tau \leq s_i & \forall i, \\ & \frac{\alpha_k}{\epsilon}(A_k x - b_k) + \frac{\alpha_k}{\epsilon}(B_k Y + C_k)\widehat{\xi}_i \\ & \quad + (1 - \frac{1}{\epsilon})\tau + \gamma_{ik}^\top(h - H\widehat{\xi}_i) \leq s_i & \forall i, k \\ & \|H^\top \gamma_{ik} - \frac{\alpha_k}{\epsilon}(B_k Y + C_k)^\top\|_* \leq \lambda & \forall i, k \\ & \gamma_{ik} \geq 0 & \forall i, k. \end{cases} \tag{8}$$

Replacing (8) into (6) completes the proof. $\qquad \square$

2. Nomenclature

In Table 1, we present the symbols used in the original paper and the description for each one of them.

Table 1. Nomenclature

Symbol	Description
p	First-stage power dispatch of conventional power plants
Y	Afine police for the second-stage dispatch of conventional power plants
$\underline{r}$	First-stage downward reserve capacity of conventional power plants
$\overline{r}$	First-stage upward reserve capacity of conventional power plants
μ	Mean power production of stochastic producers
ξ	Random variable with zero mean
W	Diagonal matrix containing the capacity of stochastic producers
Q	PDTF matrix
$r^{\max}$	Maximum reserve capacity offered by conventional power plants
$p^{\max}$	Maximum power production of conventional power plants
$p^{\min}$	Minimum power production of conventional power plants
$f^{\max}$	Capacity limit of transmission line
$q^{\max}$	Capacity limit of pipeline
Φ	Power conversion factor
d	Electricity demand
ϵ	Risk parameter of joint chance constraint
N	Number of sample data of empirical distribution
N'	Number of realizations in the training dataset
$\mathbb{P}$	True probability distribution of random variable ξ
$\widehat{\mathbb{P}}_N$	Empirical distribution of random variable ξ
$\mathcal{P}$	Ambiguity set
ρ	Wasserstein radius
$\overline{\delta}$	Upper bound of scaling parameter α
$\underline{\delta}$	Lower bound of scaling parameter α
α	Scaling parameter
η	Threshold to check the convergence of algorithm in Zymler approach
v	Auxiliary variable of algorithm in Zymler approach
$\mathbb{M}$	Big-M penalty parameter of algorithm in Zymler approach

3. Robust optimization formulation

The robust optimization formulation writes as follows,

$$
\begin{aligned}
\min_{(x,Y)\in\Theta} \quad & \widetilde{c}^\top x \;+\; \max_{\xi\in\Xi} c^\top Y\xi \\
\text{s.\,t.} \quad & A^j x + (B^j Y + C^j)\xi \le b^j \quad \forall \xi \in \Xi, \forall j,
\end{aligned}
\tag{9}
$$

where the worst-case cost is minimized and the constraints are reformulated as robust constraints in a sense that they are never violated for any realization of uncertain parameter ξ. The uncertain parameter ξ varies in $[-\mu, 1-\mu]$, which suggest to consider the box uncertainty set $\Xi = \{\xi \in \mathbb{R}^Z : -\mu_z \le \xi_z \le 1-\mu_z,\, z = 1, \ldots, Z\}$ that has 2^Z vertices. Thus, we replace each one of the constraints for each vertex ξ_v of Ξ and reformulate the objective function accordingly. The optimization problem is reformulated as follows,

$$
\begin{aligned}
\min_{x,Y,\beta} \quad & \widetilde{c}^\top x + \beta \\
\text{s.\,t.} \quad & (x,Y) \in \Theta \\
& c^\top Y\xi_v \le \beta && \forall v = 1, \ldots, 2^Z, \\
& A^j x + (B^j Y + C^j)\xi_v \le b^j && \forall v = 1, \ldots, 2^Z, \forall j
\end{aligned}
\tag{10}
$$

which is solved as a linear program.

4. Data for the IEEE 24-bus RTS

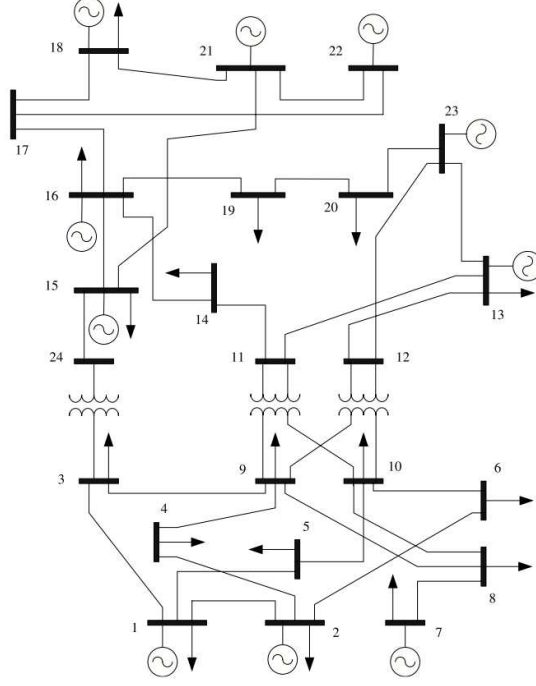The 24-bus power system is illustrated in Figure 1. The slack bus of the system is node 13.

Figure 1. 24-bus power system – Single area RTS-96

Table 2 presents the generating units' data of the power system. The generating units offer a single block of energy, up and down reserve capacity. Table 2 provides the technical data of generating units, the costs, the location on the power system, as well as the conversion factor and the connection with the corresponding pipelines for the gas-fired power plants. There are three pipelines that the gas-fired power plants are connected. Pipeline 1 has a capacity of 10 000 kcf, Pipeline 2 has a capacity of 5 500 kcf and Pipeline 3 has a capacity of 7 000 kcf (kcf: 1000 cubic feet).

Table 2. Technical Data of Generating Units

Unit #	Node	$p^{\max}$ (MW)	$p^{\min}$ (MW)	$r^{\max}$ (MW)	c ($/MWh)	$\bar{c}$ ($/MW)	$\underline{c}$ ($/MW)	Φ (kcf/MWh)	Pipeline
1	1	152	0	60.8	17.5	3.5	3.5	12.65	1
2	2	152	0	60.8	20	4	4	13.45	3
3	7	300	0	120	15	3	3	-	-
4	13	591	0	236.4	27.5	5.5	5.5	-	-
5	15	60	0	24	30	6	6	11.12	2
6	15	155	0	62	22.5	4.5	4.5	-	-
7	16	155	0	62	25	5	5	14.88	1
8	18	400	0	160	5	1	1	-	-
9	21	400	0	160	7.5	1.5	1.5	-	-
10	22	300	0	120	32.5	6.5	6.5	-	-
11	23	310	0	124	10	2	2	16.8	2
12	23	350	0	140	12.5	2.5	2.5	15.6	3

Table 3 presents the node location of the loads, as well as the load at each node as a percentage of the total system demand. The total electricity demand is 2 650 MWh and the cost of load shedding is $1 000 /MWh.

TABLE 3. Node Location and Distribution of the Total System Demand

Load #	Node	% of system load	Load #	Node	% of system load
1	1	3.8	10	10	6.8
2	2	3.4	11	13	9.3
3	3	6.3	12	14	6.8
4	4	2.6	13	15	11.1
5	5	2.5	14	16	3.5
6	6	4.8	15	18	11.7
7	7	4.4	16	19	6.4
8	8	6	17	20	4.5
9	9	6.1			

The transmission lines data is given in Table 4. The lines are characterized by the nodes that are connected, as well as the reactance and the capacity of each line.

TABLE 4. Reactance and Capacity of Transmission Lines

From	To	Reactance (p.u.)	Capacity (MW)	From	To	Reactance (p.u.)	Capacity (MW)
1	2	0.0146	175	11	13	0.0488	500
1	3	0.2253	175	11	14	0.0426	500
1	5	0.0907	400	12	13	0.0488	500
2	4	0.1356	175	12	23	0.0985	500
2	6	0.205	175	13	23	0.0884	500
3	9	0.1271	400	14	16	0.0594	1000
3	24	0.084	200	15	16	0.0172	500
4	9	0.111	175	15	21	0.0249	1000
5	10	0.094	400	15	24	0.0529	500
6	10	0.0642	400	16	17	0.0263	500
7	8	0.0652	600	16	19	0.0234	500
8	9	0.1762	175	17	18	0.0143	500
8	10	0.1762	175	17	22	0.1069	500
9	11	0.084	200	18	21	0.0132	1000
9	12	0.084	200	19	20	0.0203	1000
10	11	0.084	200	20	23	0.0112	1000
10	12	0.084	200	21	22	0.0692	500

There are 6 wind farms of 250 MW with different locations throughout the grid. The wind farms are connected at the 1, 2, 11, 12, 12, 16 nodes.

5. Reformulation of distributionally robust joint chance constraints

The positive-value vector P for the Bonferroni approximation is [0 linspace($10^{-4}, 24 \cdot 10^{-4}, 23$)], while for the Zymler approximation is given at Table 5.

TABLE 5. Positive-value Vector P for Zymler Approximation

$N = 25$	P vector
$\epsilon = 1\%$	$[0\ 10^{-4}\ \text{linspace}(10^{-3}, 10^{-2}, 23)]$
$\epsilon = 5\%$	$[0\ \text{linspace}(10^{-4}, 3.5 \cdot 10^{-2}, 24)]$
$\epsilon = 10\%$	$[0\ 10^{-4}\ 10^{-3}\ 10^{-2}\ \text{linspace}(3.5 \cdot 10^{-2}, 6 \cdot 10^{-2}, 21)]$
$N = 50$	
$\epsilon = 1\%$	$[0\ 10^{-4}\ \text{linspace}(10^{-3}, 6 \cdot 10^{-3}, 23)]$
$\epsilon = 5\%$	$[0\ 10^{-4}\ 10^{-3}\ \text{linspace}(10^{-2}, 4 \cdot 10^{-2}, 22)]$
$\epsilon = 10\%$	$[0\ 10^{-4}\ 10^{-3}\ 10^{-2}\ 3 \cdot 10^{-2}\ \text{linspace}(4 \cdot 10^{-2}, 7 \cdot 10^{-2}, 20)]$
$N = 100$	
$\epsilon = 1\%$	$[0\ 10^{-4}\ 10^{-3}\ \text{linspace}(3 \cdot 10^{-3}, 4 \cdot 10^{-2}, 22)]$
$\epsilon = 5\%$	$[0\ 10^{-4}\ 10^{-3}\ \text{linspace}(3 \cdot 10^{-3}, 4 \cdot 10^{-2}, 22)]$
$\epsilon = 10\%$	$[0\ 10^{-4}\ 10^{-3}\ 6 \cdot 10^{-3}\ \text{linspace}(10^{-2}, 6 \cdot 10^{-2}, 21)]$
$N = 200$	
$\epsilon = 1\%$	$[0\ 10^{-4}\ 10^{-3}\ \text{linspace}(3 \cdot 10^{-3}, 10^{-2}, 22)]$
$\epsilon = 5\%$	$[0\ 10^{-4}\ 10^{-3}\ \text{linspace}(3 \cdot 10^{-3}, 2.5 \cdot 10^{-2}, 22)]$
$\epsilon = 10\%$	$[0\ 10^{-4}\ 10^{-3}\ \text{linspace}(5 \cdot 10^{-3}, 4 \cdot 10^{-2}, 22)]$

Table 6 presents the values of the parameters related to the algorithm utilized in the Zymler approximation of distributionally robust joint chance constraints.

TABLE 6. Parameter for the Algorithm in Zymler Approximation

Parameter	Value
MaxIter	40
η	0.1
$\overline{\delta}$	1000
$\underline{\delta}$	10^{-4}
M	10^6

6. Additional Results

Figs. 2 and 3 illustrate the impact of Wasserstein radius ρ on the expected value and interquantile range between the 10th and 90th quantile of $\widehat{\mathcal{R}}_B^i(\rho)$. For the Bonferroni approximation, we have similar observations as the ones for Zymler approximation presented in the original manuscript.
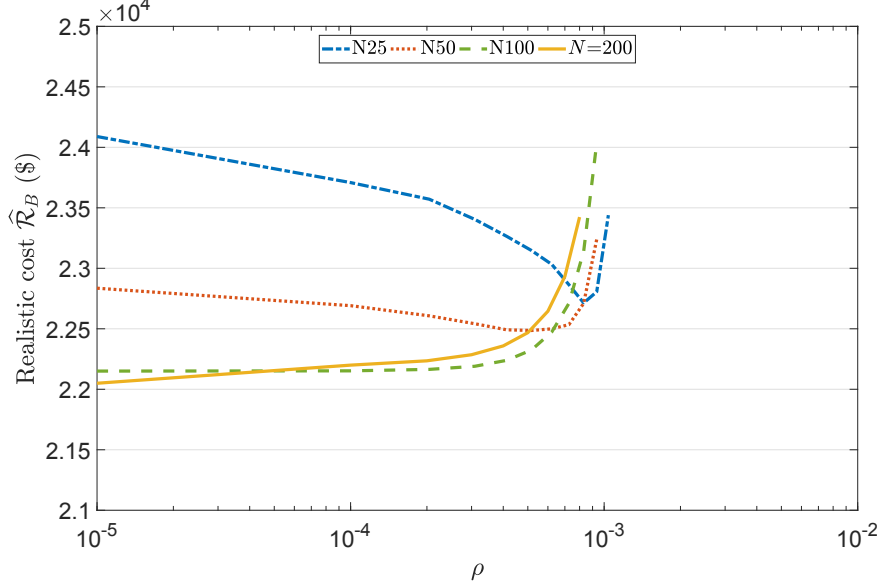

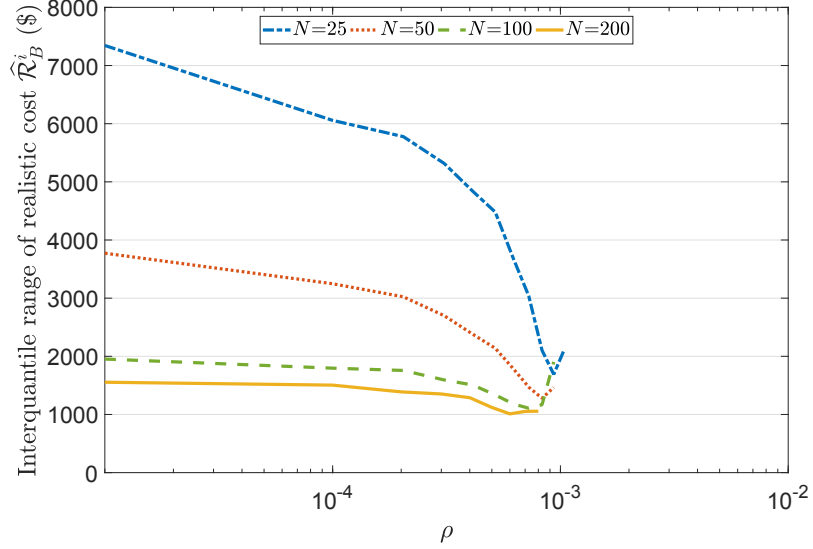FIGURE 2. Average realistic cost $\widehat{\mathcal{R}}_B$ as a function of Wasserstein radius ρ.

FIGURE 3. Interquantile range of realistic cost $\widehat{\mathcal{R}}_B^i$ between 10th and 90th quantile as a function of Wasserstein radius ρ.

References

[1] R. T. Rockafellar and S. Uryasev, "Optimization of conditional value-at-risk," *J. Risk*, vol. 2, no. 3, pp. 21–41, 2000.

[2] P. Mohajerin Esfahani and D. Kuhn, "Data-driven distributionally robust optimization using the Wasserstein metric: Performance guarantees and tractable reformulations," *Mathematical Programming*, Jul 2017.